

AD-A154 725

TWO-DIMENSIONAL QUICKEST SOLUTION OF THE DEPTH-AVERAGED  
TRANSPORT-DISPERSION EQUATION(U) ARMY ENGINEER  
WATERWAYS EXPERIMENT STATION VICKSBURG MS ENVIR.  
R W HALL ET AL. MAR 85 WES/TR/EL-85-3

1/1

UNCLASSIFIED

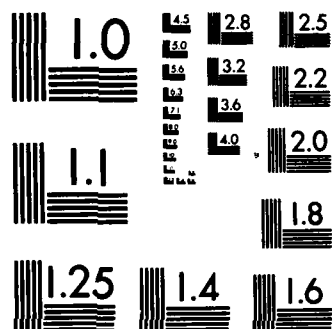
F/G 8/8

NL

END

FILMED

DTIC



MICROCOPY RESOLUTION TEST CHART  
NATIONAL BUREAU OF STANDARDS-1963-A

2

**ENVIRONMENTAL IMPACT  
RESEARCH PROGRAM**

TECHNICAL REPORT EL-85-3

**TWO-DIMENSIONAL QUICKEST  
SOLUTION OF THE DEPTH-AVERAGED  
TRANSPORT-DISPERSION EQUATION**

by

Ross W. Hall, Raymond S. Chapman

Environmental Laboratory

DEPARTMENT OF THE ARMY  
Waterways Experiment Station, Corps of Engineers  
PO Box 631, Vicksburg, Mississippi 39180-0631



March 1985

Final Report

Approved For Public Release; Distribution Unlimited

DTIC FILE COPY

**DTIC**  
**ELECTE**  
**S** JUN 12 1985 **D**

**G**

Prepared for

DEPARTMENT OF THE ARMY  
US Army Corps of Engineers  
Washington, DC 20314-1000

**85 5 15 008**

Destroy this report when no longer needed. Do not return  
it to the originator.

The findings in this report are not to be construed as an official  
Department of the Army position unless so designated  
by other authorized documents.

<b>Accession For</b>	
DTIC GRA&I	<input checked="" type="checkbox"/>
DTIC TAB	<input type="checkbox"/>
Unannounced	<input type="checkbox"/>
Justification	<input type="checkbox"/>
By _____	
Distribution/	
Availability Codes	
Dist	Avail and/or Special
A1	

The contents of this report are not to be used for  
advertising, publication, or promotional purposes.  
Citation of trade names does not constitute an  
official endorsement or approval of the use of  
such commercial products.

Unclassified

SECURITY CLASSIFICATION OF THIS PAGE (When Data Entered)

REPORT DOCUMENTATION PAGE		READ INSTRUCTIONS BEFORE COMPLETING FORM
1. REPORT NUMBER Technical Report EL-85-3	2. GOVT ACCESSION NO. <b>AD-A154725</b>	3. RECIPIENT'S CATALOG NUMBER
4. TITLE (and Subtitle) TWO-DIMENSIONAL QUICKEST; Solution of the Depth-Averaged Transport-Dispersion Equation	5. TYPE OF REPORT & PERIOD COVERED Final report	
7. AUTHOR(s) Ross W. Hall, Raymond S. Chapman	6. PERFORMING ORG. REPORT NUMBER	
9. PERFORMING ORGANIZATION NAME AND ADDRESS US Army Engineer Waterways Experiment Station Environmental Laboratory PO Box 631, Vicksburg, Mississippi 39180-0631	8. CONTRACT OR GRANT NUMBER(s)	
11. CONTROLLING OFFICE NAME AND ADDRESS DEPARTMENT OF THE ARMY US Army Corps of Engineers Washington, DC 20314-1000	10. PROGRAM ELEMENT, PROJECT, TASK AREA & WORK UNIT NUMBERS	
14. MONITORING AGENCY NAME & ADDRESS (if different from Controlling Office)	12. REPORT DATE March 1985	
	13. NUMBER OF PAGES 29	
	15. SECURITY CLASS. (of this report) Unclassified	
16. DISTRIBUTION STATEMENT (of this Report)  Approved for public release; distribution unlimited.		
17. DISTRIBUTION STATEMENT (of the abstract entered in Block 20, if different from Report)		
18. SUPPLEMENTARY NOTES  Available from National Technical Information Service, 5285 Port Royal Road, Springfield, Virginia 22161.		
19. KEY WORDS (Continue on reverse side if necessary and identify by block number) <i>cont</i> Finite Element Method, (LC) QUICKEST, (WES) Water Quality--Measurement--Mathematical Models, (LC) Diffusion--Mathematical Models, (LC)		
20. ABSTRACT (Continue on reverse side if necessary and identify by block number) → This study details the derivation of a third-order accurate, explicit, finite-difference scheme (QUICKEST) for the solution of the depth-averaged transport-dispersion equation and compares its performance to an existing third-order accurate Lagrangian algorithm (12-POINT). Test comparisons included both one- and two-dimensional transient transport. Performance criteria examined included numerical diffusion/amplitude, phase, and mass conservation errors. → <i>cont</i> <div style="text-align: right;">(Continued)</div>		

Unclassified

SECURITY CLASSIFICATION OF THIS PAGE(When Data Entered)

20. ABSTRACT (Continued).

*cont* Results presented show that both schemes possess favorable amplitude and phase characteristics. However, unlike QUICKEST, which is mass conservative, the 12-POINT scheme exhibits mass conservation errors that are directly attributable to the time step employed. Neglect of the cross-derivative terms in the QUICKEST formulation results in increased diffusion/amplitude errors as grid density decreases or time step increases.

The work presented herein is preliminary to the development of a general purpose, depth-integrated water quality model. Of the two third-order finite schemes examined, QUICKEST is far superior for engineering applications where practical grid spacing and time steps are essential.

*not keywords included* 1473

Unclassified

SECURITY CLASSIFICATION OF THIS PAGE(When Data Entered)

## PREFACE

This report was prepared under the Environmental Impact Research Program (EIRP) sponsored by the Office, Chief of Engineers (OCE), U. S. Army, Washington, D. C. Dr. John Bushman and Mr. Earl Eiker were OCE Technical Monitors. Mr. Dave Mathis was Water Resources Support Center Technical Monitor.

Authors of this report were Mr. Ross W. Hall and Dr. Raymond S. Chapman, Environmental Research and Simulation Division (ERSD), Environmental Laboratory (EL), WES. Mr. Donald L. Robey, Chief, ERSD, and Dr. John Harrison, Chief, EL, provided general supervision. Program Manager of EIRP was Dr. Roger T. Saucier, EL.

Commander and Director of WES during report preparation was COL Tilford C. Creel, CE. Technical Director was Mr. F. R. Brown.

This report should be cited as follows:

Hall, R. W., and Chapman, R. S. 1985. "Two-Dimensional QUICKEST; Solution of the Depth-Averaged Transport-Dispersion Equation," Technical Report EL-85-3, US Army Engineer Waterways Experiment Station, Vicksburg, Miss.

Accession For	
NTIS GRA&I	<input checked="checked" type="checkbox"/>
DTIC TAB	<input type="checkbox"/>
Unannounced	<input type="checkbox"/>
Justification	
By	
Date	
Avail	
Dist	
A-1	



## CONTENTS

	<u>Page</u>
PREFACE . . . . .	1
PART I: INTRODUCTION . . . . .	3
PART II: DERIVATION OF THE TWO-DIMENSIONAL QUICKEST . . . . .	5
Control Cell Formulation . . . . .	5
Cell and Cell Face Averages . . . . .	7
Approximation of the Left Hand Side . . . . .	8
Approximation of the Advective Terms . . . . .	10
Approximation of the Diffusion Terms . . . . .	12
Two-Dimensional QUICKEST Formulation . . . . .	15
PART III: THE 12-POINT SCHEME . . . . .	19
PART IV: TEST SIMULATIONS AND RESULTS . . . . .	21
One-Dimensional Advection . . . . .	21
Two-Dimensional Solid Body Rotation . . . . .	24
Neglect of the Cross-Derivative Terms . . . . .	26
PART V: CONCLUSIONS . . . . .	28
REFERENCES . . . . .	29

## TWO-DIMENSIONAL QUICKEST

### Solution of the Depth-Averaged Transport-Dispersion Equation

#### PART I: INTRODUCTION

1. The mathematical modeling of a water quality constituent in a water body frequently employs a spatial averaging in the vertical dimension to yield a depth-averaged two-dimensional transport-dispersion equation:

$$\frac{\partial(\phi h)}{\partial t} + \frac{\partial(u\phi h)}{\partial x} + \frac{\partial(v\phi h)}{\partial y} = \frac{\partial}{\partial x} \left( \Gamma_x \frac{\partial \phi h}{\partial x} \right) + \frac{\partial}{\partial y} \left( \Gamma_y \frac{\partial \phi h}{\partial y} \right) \pm S$$

where

$\phi$  = water quality constituent concentration

$h$  = water depth

$t$  = time

$u, v$  = velocity components in the  $x$ - and  $y$ -directions, respectively

$x, y$  = two-dimensional Cartesian coordinate directions

$\Gamma_x, \Gamma_y$  = dispersion coefficients in the  $x$ - and  $y$ -directions, respectively

$S$  = source and sink terms of the constituent

2. Numerous finite difference schemes have been applied to the solution of the transport-dispersion equation; however, until recently low-order spatial and temporal discretization techniques were predominately used in practical applications. Typically weighted combinations of first-order upwind and second-order central differencing were employed. Unfortunately, behavioral errors such as numerical diffusion associated with upwind differencing and the parasitic oscillations characteristic of central differencing often rendered these techniques unsuitable for applications in transport-dispersion models. Consequently, there is a need to progress to higher order schemes.

3. The relative merit of steady-state applications of spatially

third-order accurate schemes are well illustrated in the literature (Chapman and Kuo 1981; Han, Humphrey, and Launder 1981; Leonard, Leschziner, and McGuirk 1978; Leonard 1979; Leschziner 1980; Leschziner and Rodi 1981). The comparisons of the spatially third-order accurate QUICK (Quadratic Upstream Interpolation for Convective Kinematics) technique (Leonard 1979) with upwind and central differencing show QUICK to be far superior in steady transport calculations where practical grid spacings are used. However, Leonard, Leschziner, and McGuirk (1978) and Leschziner (1980) have shown that QUICK suffers from a boundedness problem when applied to transient problems. Leonard (1979), however, has presented an approximate temporally third-order accurate extension of the QUICK technique called QUICKEST (Quadratic Upstream Interpolation for Convective Kinematics with Estimated Streaming Terms), which was specifically designed to address unidirectional transient transport problems.

4. Davis and Moore (1982) presented a two-dimensional adaptation of the QUICKEST scheme. The authors stated that the neglect of the cross-derivative terms had negligible effects on the numerical results. As a consequence, the two-dimensional QUICKEST formulation of Davis and Moore (1982) is equivalent to the superposition of two unidirectional QUICKEST schemes. Results presented in this report will demonstrate that neglect of the cross-derivative terms can corrupt the solution.

5. The purpose of this report is to detail the derivation of a two-dimensional QUICKEST scheme and compare its performance to an existing third-order accurate Lagrangian algorithm of Hinstrupt, Kej, and Kroszynski (1977) referred to in this report as the 12-POINT scheme. Test comparisons included both one- and two-dimensional transient transport. Performance criteria examined included numerical diffusion/amplitude, phase, and mass conservation errors.

6. Part II of this report details the derivation of the two-dimensional QUICKEST. Part III summarizes the 12-POINT scheme used in the comparison. Part IV describes the one- and two-dimensional test cases employed and summarizes the results of the comparisons.

## PART II: DERIVATION OF THE TWO-DIMENSIONAL QUICKEST

7. The two-dimensional version of QUICKEST is an extension of the one-dimensional work of Leonard (1979). The derivation of QUICKEST is based on a conservative control cell formulation and uses a spatial six-point upstream weighted interpolation surface with temporal advective correction to obtain third-order approximations to cell and cell face averaged quantities.

### Control Cell Formulation

8. The depth-averaged transport-dispersion equation with source and sink terms neglected

$$\frac{\partial(\phi h)}{\partial t} + \frac{\partial(u\phi h)}{\partial x} + \frac{\partial(v\phi h)}{\partial y} = \frac{\partial}{\partial x} \left( \Gamma_x \frac{\partial \phi h}{\partial x} \right) + \frac{\partial}{\partial y} \left( \Gamma_y \frac{\partial \phi h}{\partial y} \right) \quad (1)$$

is integrated over a control cell on a constant space, square, computational grid (Figure 1) and in time. For convenience, the depth-averaged scalar,  $\phi h$ , will henceforth be designated as  $\phi$ . The exact integral formulation is written:

$$\int_{-\Delta y/2}^{\Delta y/2} \int_{-\Delta x/2}^{\Delta x/2} (\phi^{n+1} - \phi^n) dx dy \quad (2a)$$

$$= -\Delta y \int_0^{\Delta t} (u_R \phi_R - u_L \phi_L) dt - \Delta x \int_0^{\Delta t} (v_T \phi_T - v_B \phi_B) dt \quad (2b)$$

$$= + \Delta y \int_0^{\Delta t} \left[ \left( \Gamma \frac{\partial \phi}{\partial x} \right)_R - \left( \Gamma \frac{\partial \phi}{\partial x} \right)_L \right] dt + \Delta x \int_0^{\Delta t} \left[ \left( \Gamma \frac{\partial \phi}{\partial y} \right)_T - \left( \Gamma \frac{\partial \phi}{\partial y} \right)_B \right] dt \quad (2c)$$

in which the superscripts  $n$  and  $n+1$  denote time levels and the subscripts  $R$ ,  $L$ ,  $T$ , and  $B$  denote right, left, top, and bottom cell face averages, respectively.

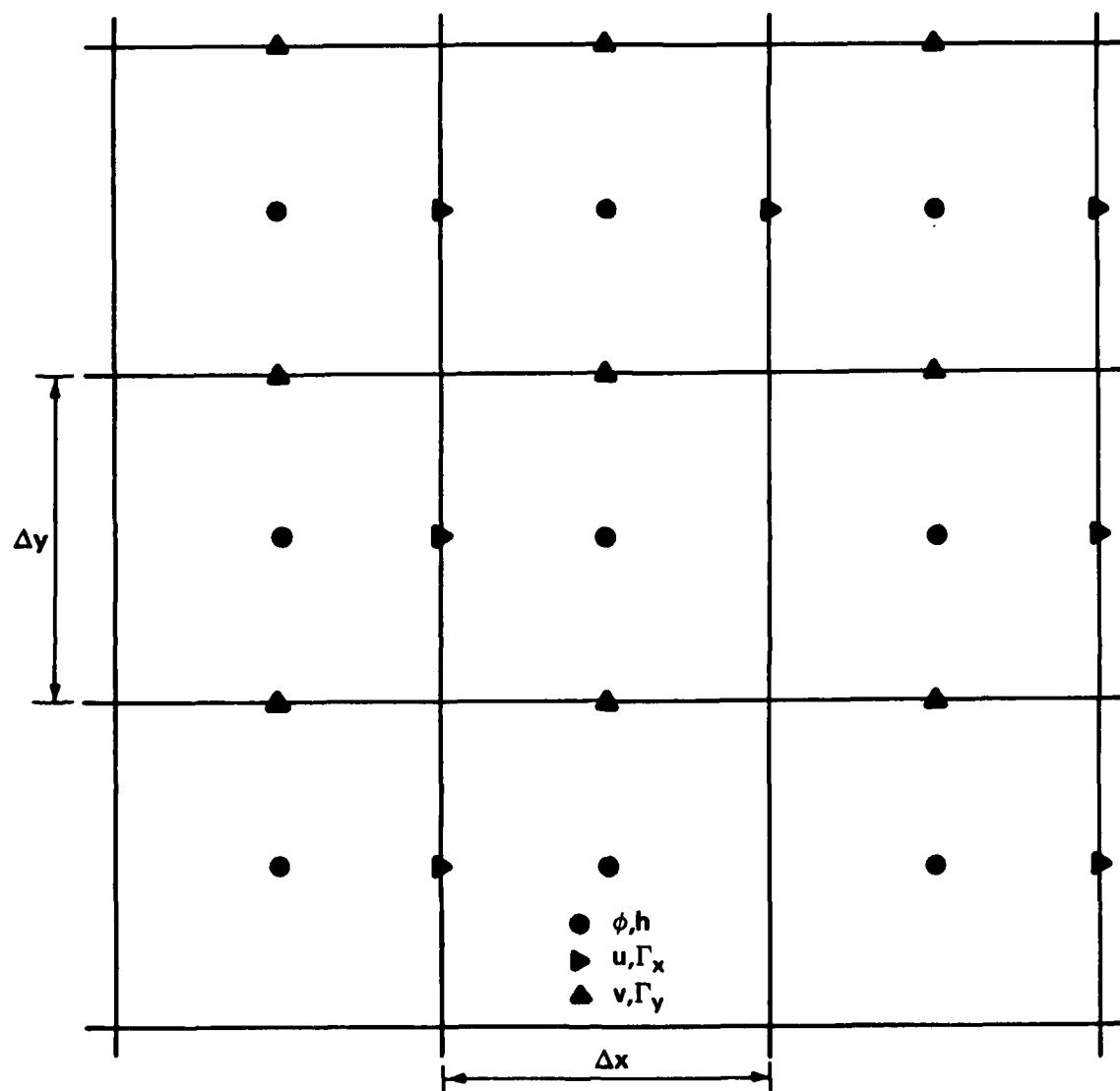


Figure 1. Computational grid and definition of variables. Nodal values represent cell averages; cell wall values represent cell wall averages

### Cell and Cell Face Averages

9. A key feature of QUICKEST is the use of a spatial six-point upstream weighted interpolation surface to spatially estimate cell and cell face averages. To illustrate the procedure, the computation is demonstrated for the right cell face average using the information presented in Figure 2. The  $u$  and  $v$  velocity components are positive.

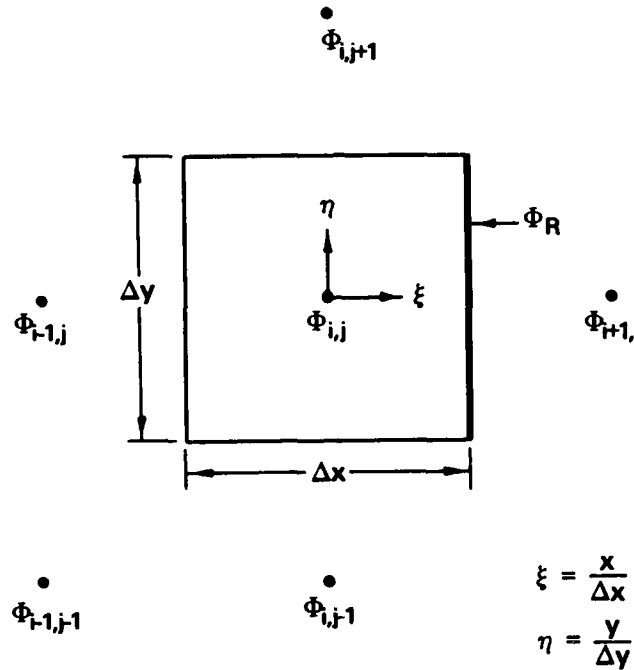


Figure 2. Estimation of right cell face average  $\phi_R$ , given  $u, v > 0$

10. Specifying a Gauss backward difference interpolation formula in the longitudinal  $\xi$  and transverse  $\eta$  direction, a quadratic interpolation function can be written at  $x = i\Delta x$ ,  $y = j\Delta y$  (Hildebrand 1956):

$$\phi_{\xi, \eta} = \left[ 1 + \xi \nabla_{\xi} + \frac{\xi(\xi + 1)}{2} \delta_{\xi}^2 + \eta \nabla_{\eta} + \xi \eta \nabla_{\xi} \nabla_{\eta} + \frac{\eta(\eta + 1)}{2} \delta_{\eta}^2 \right] \phi_{i,j} \quad (3)$$

where  $\xi = x/\Delta x$  and  $\eta = y/\Delta y$  are local nondimensional coordinates,  $\nabla$  is the backward difference operator, and  $\delta$  is the central differences operator.

11. The right cell face average is then computed as follows:

$$\phi_R = \int_{-1/2}^{1/2} \phi_{1/2,\eta} d\eta = \frac{1}{2} (\phi_{i,j} + \phi_{i+1,j}) - \frac{\delta_x^2}{8} \phi_{i,j} + \frac{\delta_y^2}{24} \phi_{i,j}$$

12. For negative transverse velocities, the transverse correction term,  $\delta_y^2/24$ , remains the same. However, for negative longitudinal velocities, the appropriate cell face average is computed:

$$\phi_R = \frac{1}{2} (\phi_{i,j} + \phi_{i+1,j}) - \frac{\delta_x^2}{8} \phi_{i+1,j} + \frac{\delta_y^2}{24} \phi_{i+1,j}$$

#### Approximation of the Left Hand Side (LHS)

13. The evaluation of the LHS (Equation 2a) consists of approximating the cell average at each time level by a quadratic interpolation surface, integrating over the appropriate limits, and spatially approximating temporal gradients.

14. Substituting the quadratic interpolation function (3) into term (2a), the LHS is written:

$$\begin{aligned} \int_{-\Delta y/2}^{\Delta y/2} \int_{-\Delta x/2}^{\Delta x/2} (\phi^{n+1} - \phi^n) dx dy &= \Delta x \Delta y \int_{-1/2}^{1/2} \int_{-1/2}^{1/2} (\phi_{\xi,\eta}^{n+1} - \phi_{\xi,\eta}^n) d\xi d\eta \\ &= \Delta x \Delta y \left( 1 + \frac{\delta_x^2}{24} + \frac{\delta_y^2}{24} \right) (\phi_{i,j}^{n+1} - \phi_{i,j}^n) \\ &= \Delta x \Delta y \left[ \phi_{i,j}^{n+1} - \phi_{i,j}^n + \frac{\delta_x^2}{24} (\phi_{i,j}^{n+1} - \phi_{i,j}^n) + \frac{\delta_y^2}{24} (\phi_{i,j}^{n+1} - \phi_{i,j}^n) \right] \end{aligned}$$

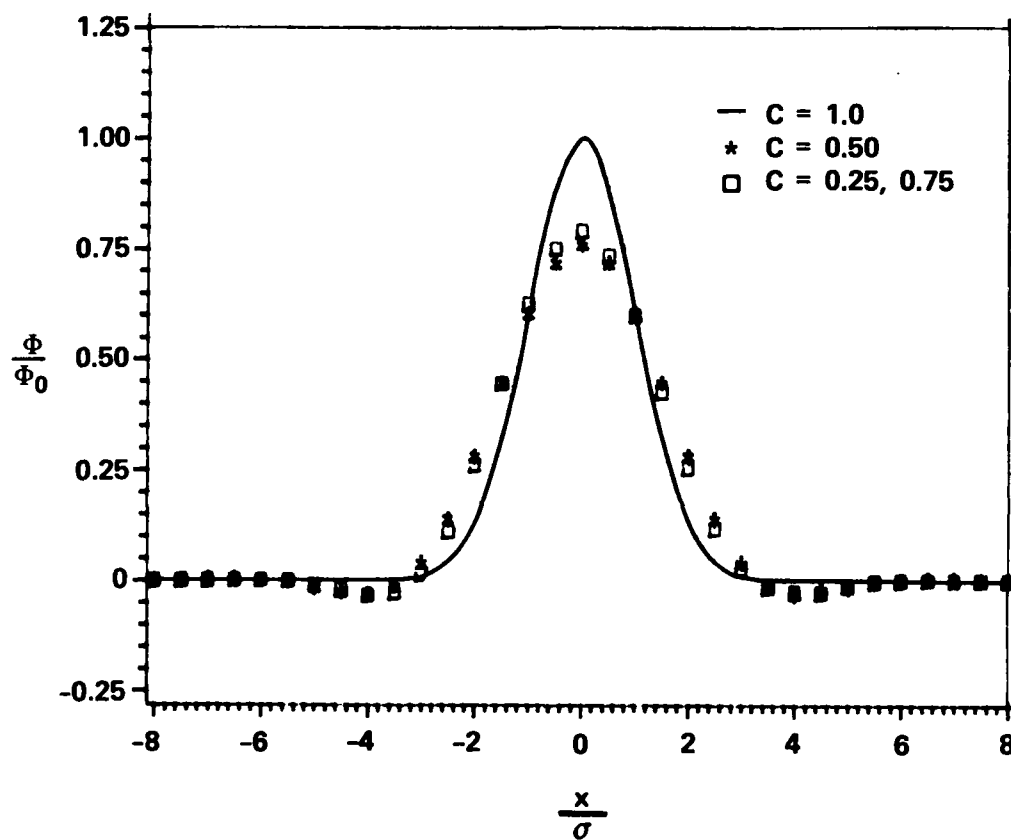


Figure 5. Effects of Courant numbers on the unidirectional advection of a Gaussian ( $\sigma = 2\Delta x$ ) distribution

## PART IV: TEST SIMULATIONS AND RESULTS

31. A systematic program of numerical experimentation was performed in two phases. The first phase consisted of the advection of a Gaussian distribution in a uniform velocity field in one dimension. The second phase consisted of the solid body rotation of a Gaussian distribution.

### One-Dimensional Advection

32. For spatially constant Courant numbers and no diffusion, QUICKEST and 12-POINT are algebraically equivalent in one dimension. Therefore, results presented for the unidirectional advection tests are applicable to both QUICKEST and 12-POINT.

33. The unidirectional advection of a Gaussian distribution was conducted at Courant numbers ( $u\Delta t/\Delta x$ ) of 0.25, 0.50, 0.75, and 1.0. Each test computation was run for 200 time steps. In addition, grid density effects were investigated by distributing 95 percent of the initial distribution over 5, 9, or 17 grid points, which corresponds to variances of  $(\Delta x)^2$ ,  $4(\Delta x)^2$ , and  $16(\Delta x)^2$ , respectively.

34. Figure 5 presents the results for an initial Gaussian distribution of variance  $4(\Delta x)^2$  and varying Courant numbers. Examination of the figure reveals negligible phase error; however, a noticeable but slight amplitude difference is seen between Courant numbers 0.5 and 0.25/0.75.

35. The large amplitude differences observed between Courant number 1.0, which reproduces the continuum solution through exact point-to-point transport, and Courant numbers 0.25, 0.50, and 0.75 are due to the grid density selected. Figure 6 is a comparison of model simulations performed at a Courant number equal to 0.5 for varying grid density. This figure clearly demonstrates the importance of selecting an appropriate grid density.

The function on the right hand side is approximated by a 12-point, two-dimensional Everett quadratic interpolation function:

$$\begin{aligned}\phi_{i,j}^{n+1} = & (1-r)(1-s) \left[ 1 - \frac{r(2-r)}{6} \delta_x^2 - \frac{s(2-s)}{6} \delta_y^2 \right] \phi_{i,j}^n \\ & + r(1-s) \left[ 1 - \frac{1-r^2}{6} \delta_x^2 - \frac{s(2-s)}{6} \delta_y^2 \right] \phi_{i+1,j}^n \\ & + (1-r)s \left[ 1 - \frac{r(2-r)}{6} \delta_x^2 - \frac{1-s^2}{6} \delta_y^2 \right] \phi_{i,j+1}^n \\ & + rs \left( 1 - \frac{1-r^2}{6} \delta_x^2 - \frac{1-s^2}{6} \delta_y^2 \right) \phi_{i+1,j+1}^n\end{aligned}$$

Where  $r$  and  $s$  are local coordinates and  $\delta^2$  is the second central difference operator.

$$r = \frac{x - u\Delta t}{\Delta x}$$

$$s = \frac{y - v\Delta t}{\Delta y}$$

$$\delta_x^2 \phi_{i,j} = \phi_{i-1,j} - 2\phi_{i,j} + \phi_{i+1,j}$$

30. The second stage uses second central differences to approximate the dispersion terms using the nodal values updated during the first stage.

### PART III: THE 12-POINT SCHEME

28. The 12-POINT scheme uses grid and variable definitions equivalent to those used in the QUICKEST formulation except that velocities are defined at nodal points; spatially represents a cell average; and temporally represents an average over the time interval  $(0, \Delta t)$ .

29. For each time step, two computational stages are performed: a pure advective transport stage followed by a dispersion stage. For the first stage, the value of the scalar at the node labeled  $\phi$  at the  $n+1$  time level in Figure 4 is equal to the scalar at the point

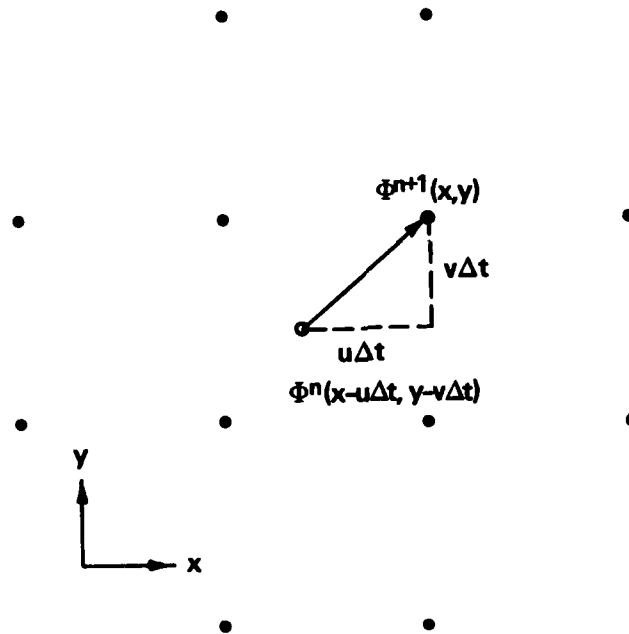


Figure 4. The 12-POINT Lagrangian procedure

labeled  $\phi$  at  $n$  time level.  $\phi^{n+1}$  is located upstream from  $\phi^n$  a distance  $\bar{v}\Delta t$  where  $\bar{v}$  represents the velocity vector. In algebraic notation, the relation is written:

$$\phi^{n+1}(x,y) = \phi^n(x - u\Delta t, y - v\Delta t)$$

$$\begin{aligned}
& - \alpha_R \left( \Delta_x \phi_{i,j}^n - \frac{C_R}{2} \delta_x^2 \phi_{i,j}^n - \frac{C_{TR}}{2} \delta_{xy}^2 \phi_{i+1/2,j-1/2}^n \right) \\
F_T = & C_T \left\{ \frac{1}{2} \left( \phi_{i,j}^n + \phi_{i,j+1}^n \right) - \frac{C_T}{2} \Delta_y \phi_{i,j}^n + \left[ \frac{\alpha_T}{2} - \frac{1}{6} (1 - C_T^2) \right] \delta_y^2 \phi_{i,j}^n \right. \\
& \left. - \frac{C_{RT}}{2} \Delta_x \phi_{i-1,j}^n + \left( \frac{\alpha_{RT}}{2} + \frac{C_{RT}^2}{6} \right) \delta_x^2 \phi_{i,j}^n + \frac{C_T C_{RT}}{3} \delta_{xy}^2 \phi_{i-1/2,j+1/2}^n \right\} \\
& - \alpha_T \left( \Delta_y \phi_{i,j}^n - \frac{C_T}{2} \delta_y^2 \phi_{i,j}^n - \frac{C_{RT}}{2} \delta_{xy}^2 \phi_{i-1/2,j+1/2}^n \right)
\end{aligned}$$

The advective and diffusive contributions through the top cell face are written:

$$\begin{aligned}
 F_T = C_T & \left[ \frac{1}{2} (\phi_{i,j}^n + \phi_{i,j+1}^n) - \frac{C_T}{2} \Delta_y \phi_{i,j}^n + \frac{C_T^2}{6} \delta_y^2 \phi_{i,j+1/2}^n \right. \\
 & - \frac{1}{8} \delta_y^2 \phi_{i,j}^n - \frac{1}{24} \delta_y^2 \phi_{i,j+1/2}^n + \frac{\alpha_T}{2} \delta_y^2 \phi_{i,j+1/2}^n + \frac{\alpha_{RT}}{2} \delta_x^2 \phi_{i,j+1/2}^n \\
 & + \frac{1}{24} \delta_x^2 \phi_{i,j}^n - \frac{1}{24} \delta_x^2 \phi_{i,j+1/2}^n - \frac{C_{RT}}{2} \Delta_x \phi_{i-1/2,j+1/2}^n + \frac{C_{RT}^2}{6} \delta_x^2 \phi_{i,j+1/2}^n \\
 & \left. + \frac{C_T C_{RT}}{3} \delta_{xy}^2 \phi_{i,j+1/2}^n - \alpha_T \left( \Delta_y \phi_{i,j}^n - \frac{C_T}{2} \delta_y^2 \phi_{i,j+1/2}^n - \frac{C_{RT}}{2} \delta_{xy}^2 \phi_{i,j+1/2}^n \right) \right] \quad (15b)
 \end{aligned}$$

where

$$\alpha_T = \frac{\Gamma_R \Delta t}{\Delta x^2} \quad \alpha_{RT} = \frac{\Gamma_{RT} \Delta t}{\Delta x^2}$$

$$\alpha_T = \frac{\Gamma_T \Delta t}{\Delta y^2} \quad \alpha_{TR} = \frac{\Gamma_{TR} \Delta t}{\Delta y^2}$$

27. Examination of expressions 15a and 15b reveals that many of the finite difference operators are centered on cell faces and not nodal points. Shifting these operators upstream one-half increment, the flux expressions are written:

$$\begin{aligned}
 F_R = C_R & \left\{ \frac{1}{2} (\phi_{i,j}^n + \phi_{i+1,j}^n) - \frac{C_R}{2} \Delta_x \phi_{i,j}^n + \left[ \frac{\alpha_R}{2} - \frac{1}{6} (1 - C_R^2) \right] \delta_x^2 \phi_{i,j}^n \right. \\
 & \left. - \frac{C_{TR}}{2} \Delta_y \phi_{i,j-1}^n + \left( \frac{\alpha_{TR}}{2} + \frac{C_{TR}^2}{6} \right) \delta_y^2 \phi_{i,j}^n + \frac{C_R C_{TR}}{3} \delta_{xy}^2 \phi_{i+1/2,j-1/2}^n \right\}
 \end{aligned}$$

$$\begin{aligned}
\text{LHS} = \Delta x \Delta y & \left( \phi_{i,j}^{n+1} - \phi_{i,j}^n \right. \\
& - \frac{\hat{C}_R}{24} \delta_x^2 \phi_{i+1/2,j} - \frac{\hat{C}_R}{24} \delta_y^2 \phi_{i+1/2,j} \quad (\text{Right Cell Face}) \\
& + \frac{\hat{C}_L}{24} \delta_x^2 \phi_{i-1/2,j} + \frac{\hat{C}_L}{24} \delta_y^2 \phi_{i-1/2,j} \quad (\text{Left Cell Face}) \\
& - \frac{\hat{C}_T}{24} \delta_y^2 \phi_{i,j+1/2} - \frac{\hat{C}_T}{24} \delta_x^2 \phi_{i,j+1/2} \quad (\text{Top Cell Face}) \\
& \left. + \frac{\hat{C}_B}{24} \delta_y^2 \phi_{i,j-1/2} + \frac{\hat{C}_B}{24} \delta_x^2 \phi_{i,j-1/2} \right) \quad (\text{Bottom Cell Face})
\end{aligned}$$

26. Equating the LHS and right hand side (RHS), the flux through the right cell face, given positive  $u$  and  $v$  velocity components, is written:

$$\begin{aligned}
F_R = C_R & \left[ \frac{1}{2} (\phi_{i,j}^n + \phi_{i+1,j}^n) - \frac{C_R}{2} \Delta_x \phi_{i,j}^n + \frac{C_R^2}{6} \delta_x^2 \phi_{i+1/2,j}^n \right. \\
& - \frac{1}{8} \delta_x^2 \phi_{i,j}^n - \frac{1}{24} \delta_x^2 \phi_{i+1/2,j}^n + \frac{\alpha_R}{2} \delta_x^2 \phi_{i+1/2,j}^n + \frac{\alpha_{TR}}{2} \delta_y^2 \phi_{i+1/2,j}^n \\
& + \frac{1}{24} \delta_y^2 \phi_{i,j}^n - \frac{1}{24} \delta_y^2 \phi_{i+1/2,j}^n - \frac{C_{TR}}{2} \Delta_y \phi_{i+1/2,j-1/2}^n + \frac{C_{TR}^2}{6} \delta_y^2 \phi_{i+1/2,j}^n \\
& \left. + \frac{C_R C_{TR}}{3} \delta_{xy}^2 \phi_{i+1/2,j}^n \right] - \alpha_R \left( \Delta_x \phi_{i,j}^n - \frac{C_R}{2} \delta_x^2 \phi_{i+1/2,j}^n - \frac{C_{TR}}{2} \delta_{xy}^2 \phi_{i+1/2,j}^n \right)
\end{aligned} \tag{15a}$$

23. From the definition of the advective transport equation:

$$\frac{\partial \phi}{\partial t} = -u \frac{\partial \phi}{\partial x} - v \frac{\partial \phi}{\partial y} + \text{H.O.T.} \quad (14)$$

Substituting Equation 14 into 13:

$$\Delta_x \phi_{i,j}^n - \frac{1}{2} \frac{\partial}{\partial x} \left( u \frac{\partial \phi}{\partial x} \right) \Delta t \Delta x - \frac{1}{2} \frac{\partial}{\partial x} \left( v \frac{\partial \phi}{\partial y} \right) \Delta t \Delta x$$

Assuming that  $u$  and  $v$  are approximately constant, the expression is written:

$$\Delta_x \phi_{i,j}^n - \frac{1}{2} u \Delta t \Delta x \frac{\partial^2 \phi}{\partial x^2} - \frac{1}{2} v \Delta t \Delta x \frac{\partial^2 \phi}{\partial x \partial y}$$

$$\Delta_x \phi_{i,j}^n - \frac{1}{2} C_R \delta_{x,i+1/2,j}^2 \phi_{i+1/2,j}^n - \frac{C_{TR}}{2} \delta_{xy}^2 \phi_{i+1/2,j}^n$$

The diffusive flux through the right cell face is written:

$$\frac{\Delta t \Delta y \Gamma_R}{\Delta x} \left( \Delta_x \phi_{i,j}^n - \frac{1}{2} C_R \delta_{x,i+1/2,j}^2 \phi_{i+1/2,j}^n - \frac{C_{TR}}{2} \delta_{xy}^2 \phi_{i+1/2,j}^n \right)$$

#### Two-Dimensional QUICKEST Formulation

24. The QUICKEST formulation of the depth-integrated transport-dispersion equation is written:

$$\phi_{i,j}^{n+1} = \phi_{i,j}^n - F_R + F_L - F_T + F_B$$

where  $F_R$ ,  $F_L$ ,  $F_T$ , and  $F_B$  represent advective and diffusive contributions through the right, left, top, and bottom cell faces, respectively.

25. In Equation 9 a caret was used to denote the assumption of approximately constant velocity. It is necessary to assign a cell face designation in order to simplify the advective transport equation. Rearranging the LHS (Equation 9):

$$\int_0^{\Delta t} \left( \frac{\partial \Phi}{\partial x} \right)_x dt = \frac{\Delta t}{\Delta x} \int_0^1 \left( \frac{\partial \Phi}{\partial r} \right)_r ds$$

Evaluating at  $r = \frac{1}{2}$  :

$$\begin{aligned} \left( \frac{\partial \Phi}{\partial r} \right)_{1/2} &= (\Delta r + s \Delta_r \Delta_s) f_{o,o} \Big|_{1/2} \\ &= (\Delta_r + s \Delta_r \Delta_s) f_{o,o} \end{aligned}$$

Integrating  $s$  on  $(0,1)$  :

$$\begin{aligned} \int_0^1 \left( \frac{\partial \Phi}{\partial r} \right)_{1/2} ds &= \left( \Delta_r + \frac{1}{2} \Delta_r \Delta_s \right) f_{o,o} \\ &= \Delta_x \phi_{i,j}^n + \frac{1}{2} \left( \Delta_x \phi_{i,j}^{n+1} - \Delta_x \phi_{i,j}^n \right) \end{aligned} \quad (12)$$

where

$$\Delta_x \phi_{i,j}^n = \phi_{i+1,j}^n - \phi_{i,j}^n$$

Recognizing that

$$\Delta_x \phi_{i,j}^n \approx \frac{\partial \Phi}{\partial x} \Delta x$$

$$\left( \frac{\partial \Phi}{\partial x} \right)^{n+1} \Delta x - \left( \frac{\partial \Phi}{\partial x} \right)^n \Delta x \approx \frac{\partial}{\partial t} \left( \frac{\partial \Phi}{\partial x} \right) \Delta t \Delta x$$

Equation 12 is written:

$$\Delta_x \phi_{i,j}^n + \frac{1}{2} \frac{\partial}{\partial t} \left( \frac{\partial \Phi}{\partial x} \right) \Delta t \Delta x = \Delta_x \phi_{i,j}^n + \frac{1}{2} \frac{\partial}{\partial x} \left( \frac{\partial \Phi}{\partial t} \right) \Delta t \Delta x \quad (13)$$

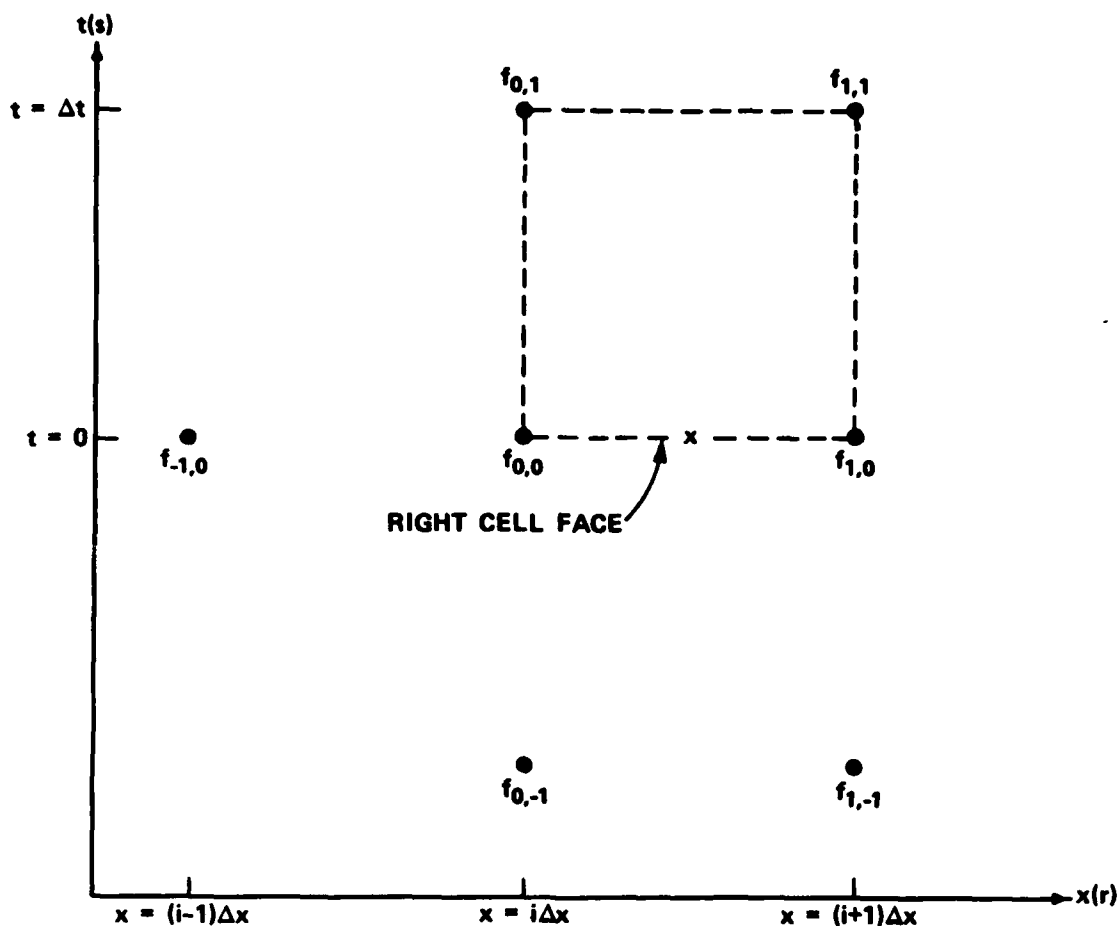


Figure 3. Definition of interpolation surface to estimate the diffusive flux through the right cell face

and the time interval on  $t \in (0,1)$  (Figure 3). Specifying Newton forward difference interpolation formulas in both  $r$  and  $s$ , a quadratic interpolation function can be written (Hildebrand 1956):

$$f_{r,s} = \left[ 1 + r\Delta_r + \frac{r(r-1)}{2} \Delta_r^2 + sr\Delta_r\Delta_s + s\Delta_s + \frac{s(s-1)}{2} \Delta_s^2 \right] f_{0,0}$$

where  $r = \frac{x}{\Delta x}$ ,  $s = \frac{t}{\Delta t}$ , and  $\Delta$  is the forward difference operator.

22. Note that following transformation of coordinates

Substituting these definitions into Equation 10, the advective flux is written:

$$\begin{aligned}
 \Delta y \int_0^{\Delta t} u_R \phi_R dt &= \Delta y \Delta x C_R \left[ \phi_R^n + \frac{\Delta t}{2} \left( -u \frac{\partial \phi}{\partial x} - v \frac{\partial \phi}{\partial y} + \Gamma_x \frac{\partial^2 \phi}{\partial x^2} + \Gamma_y \frac{\partial^2 \phi}{\partial y^2} \right) \right. \\
 &+ \left. \frac{\Delta t^2}{6} \left( u^2 \frac{\partial^2 \phi}{\partial x^2} + 2uv \frac{\partial^2 \phi}{\partial x \partial y} + v^2 \frac{\partial^2 \phi}{\partial y^2} \right) \right] \approx \Delta y \Delta x C_R \left[ \phi_R^n - \frac{C_R}{2} \Delta_x \phi_{i,j}^n \right. \\
 &- \frac{C_{TR}}{2} \Delta_y \phi_{i+1/2,j-1/2}^n + \frac{\Gamma_x \Delta t}{2 \Delta x^2} \delta_x^2 \phi_{i+1/2,j}^n + \frac{\Gamma_y \Delta t}{2 \Delta y^2} \delta_y^2 \phi_{i+1/2,j}^n \\
 &\left. + \frac{C_R^2}{6} \delta_x^2 \phi_{i+1/2,j}^n + \frac{C_{TR}^2}{6} \delta_y^2 \phi_{i+1/2,j}^n + \frac{C_R C_{TR}}{3} \delta_{xy}^2 \phi_{i+1/2,j}^n \right] \quad (11)
 \end{aligned}$$

where

$$\phi_R^n = \frac{1}{2} (\phi_{i,j}^n + \phi_{i+1,j}^n) - \frac{1}{8} \delta_x^2 \phi_{i,j}^n + \frac{1}{24} \delta_y^2 \phi_{i,j}^n$$

#### Approximation of the Diffusion Terms

19. To illustrate the procedure, the computation is demonstrated for the right cell face with both  $u$  and  $v$  velocity components positive (Figure 3).

20. The integral

$$\Delta y \int_0^{\Delta t} \left( \Gamma \frac{\partial \phi}{\partial x} \right)_R dt = \Delta y \Gamma_R \int_0^{\Delta t} \left( \frac{\partial \phi}{\partial x} \right)_R dt$$

represents the diffusive flux through the right cell face over the time interval  $(0, \Delta t)$ .

21. Construct a two-dimensional interpolation function  $(x, t) \rightarrow (r, s)$  such that the right cell face can be examined on  $x \in (-\Delta x/2, \Delta x/2)$

for the right cell face with both  $u$  and  $v$  velocity components positive.

17. The integral

$$\Delta y \int_0^{\Delta t} u_R \phi_R dt$$

represents the advective mass flux through the right cell face during the time interval  $(0, \Delta t)$ . Evaluation of the integral requires that  $u_R$  and  $\phi_R$  be known as functions of time.

18. As an approximation assume that  $u_R$  is approximately constant over the time interval

$$\Delta y u_R \int_0^{\Delta t} \phi_R dt$$

Expand the integrand in a Taylor series about  $t = 0$

$$\Delta y u_R \int_0^{\Delta t} \left[ \phi_R \Big|_0 + t \frac{\partial \phi}{\partial t} \Big|_0 + \frac{t^2}{2} \frac{\partial^2 \phi}{\partial t^2} \Big|_0 + \text{H.O.T.} \right] dt$$

Integrating

$$\Delta y u_R \left( \Delta t \phi_R + \frac{\Delta t^2}{2} \frac{\partial \phi}{\partial t} + \frac{\Delta t^3}{6} \frac{\partial^2 \phi}{\partial t^2} \right) = \Delta y \Delta x C_R \left( \phi_R + \frac{\Delta t}{2} \frac{\partial \phi}{\partial t} + \frac{\Delta t^2}{6} \frac{\partial^2 \phi}{\partial t^2} \right) \quad (10)$$

From the definition of the advective transport equation

$$\frac{\partial \phi}{\partial t} = -u \frac{\partial \phi}{\partial x} - v \frac{\partial \phi}{\partial y} + \Gamma_x \frac{\partial^2 \phi}{\partial x^2} + \Gamma_y \frac{\partial^2 \phi}{\partial y^2}$$

$$\frac{\partial^2 \phi}{\partial t^2} = u^2 \frac{\partial^2 \phi}{\partial x^2} + 2uv \frac{\partial^2 \phi}{\partial x \partial y} + v^2 \frac{\partial^2 \phi}{\partial y^2} + \text{H.O.T.}$$

Recognizing that

$$\frac{\partial}{\partial x} \left( \frac{\partial^2 \phi}{\partial x^2} \right) \approx \frac{\delta_x^2 \phi_{i+1/2,j} - \delta_x^2 \phi_{i-1/2,j}}{\Delta x^3}$$

and similar relations for  $\frac{\partial}{\partial x} \left( \frac{\partial^2 \phi}{\partial y^2} \right)$ ,  $\frac{\partial}{\partial y} \left( \frac{\partial^2 \phi}{\partial x^2} \right)$ , and  $\frac{\partial}{\partial y} \left( \frac{\partial^2 \phi}{\partial y^2} \right)$ ,

Equation 7 is written:

$$\begin{aligned} \text{LHS} = \Delta x \Delta y \left\{ \phi_{i,j}^{n+1} - \phi_{i,j}^n + \frac{\Delta t}{24} \left[ -\frac{u}{\Delta x} (\delta_x^2 \phi_{i+1/2,j} - \delta_x^2 \phi_{i-1/2,j}) \right. \right. \\ \left. \left. - \frac{v}{\Delta y} (\delta_x^2 \phi_{i,j+1/2} - \delta_x^2 \phi_{i,j-1/2}) \right] + \frac{\Delta t}{24} \left[ -\frac{u}{\Delta x} (\delta_y^2 \phi_{i+1/2,j} \right. \right. \\ \left. \left. - \delta_y^2 \phi_{i-1/2,j}) - \frac{v}{\Delta y} (\delta_y^2 \phi_{i,j+1/2} - \delta_y^2 \phi_{i,j-1/2}) \right] \right\} \quad (8) \end{aligned}$$

Recognizing the Courant numbers  $\hat{C}_x = \frac{u \Delta t}{\Delta x}$  and  $\hat{C}_y = \frac{v \Delta t}{\Delta y}$  and using the caret to denote the approximations in Equation 6, the LHS is written:

$$\begin{aligned} \text{LHS} = \Delta x \Delta y \left[ \phi_{i,j}^{n+1} - \phi_{i,j}^n - \frac{\hat{C}_x}{24} (\delta_x^2 \phi_{i+1/2,j} - \delta_x^2 \phi_{i-1/2,j}) \right. \\ \left. - \frac{\hat{C}_y}{24} (\delta_x^2 \phi_{i,j+1/2} - \delta_x^2 \phi_{i,j-1/2}) - \frac{\hat{C}_x}{24} (\delta_y^2 \phi_{i+1/2,j} - \delta_y^2 \phi_{i-1/2,j}) \right. \\ \left. - \frac{\hat{C}_y}{24} (\delta_y^2 \phi_{i,j+1/2} - \delta_y^2 \phi_{i,j-1/2}) \right] \quad (9) \end{aligned}$$

#### Approximation of the Advective Terms

16. To illustrate the procedure, the computation is demonstrated

recognizing that

$$\delta_x^2 \phi_{i,j} \approx \Delta x^2 \frac{\partial^2 \phi}{\partial x^2}$$

$$\delta_y^2 \phi_{i,j} \approx \Delta y^2 \frac{\partial^2 \phi}{\partial y^2}$$

$$\phi^{n+1} - \phi^n \approx \Delta t \frac{\partial \phi}{\partial t}$$

the LHS is written:

$$\text{LHS} = \Delta x \Delta y \left[ \phi_{i,j}^{n+1} - \phi_{i,j}^n + \left( \frac{\Delta t \Delta x^2}{24} \right) \frac{\partial}{\partial t} \left( \frac{\partial^2 \phi}{\partial x^2} \right) + \left( \frac{\Delta t \Delta y^2}{24} \right) \frac{\partial}{\partial t} \left( \frac{\partial^2 \phi}{\partial y^2} \right) \right] \quad (4)$$

15. Differentiating and rearranging, the depth-integrated transport-dispersion equation (1) is written:

$$\begin{aligned} \frac{\partial}{\partial t} \left( \frac{\partial^2 \phi}{\partial x^2} \right) &= - \frac{\partial}{\partial x} \left( \frac{\partial^2 u \phi}{\partial x^2} \right) - \frac{\partial}{\partial y} \left( \frac{\partial^2 v \phi}{\partial x^2} \right) + \text{H.O.T.} \\ \frac{\partial}{\partial t} \left( \frac{\partial^2 \phi}{\partial y^2} \right) &= - \frac{\partial}{\partial x} \left( \frac{\partial^2 u \phi}{\partial y^2} \right) - \frac{\partial}{\partial y} \left( \frac{\partial^2 v \phi}{\partial y^2} \right) + \text{H.O.T.} \end{aligned} \quad (5)$$

where H.O.T. represents the higher order terms. Assume  $u$  and  $v$  are approximately constant between adjacent cell faces:

$$\begin{aligned} \frac{\partial(u\phi)}{\partial x} &\approx u \frac{\partial \phi}{\partial x} \\ \frac{\partial(v\phi)}{\partial y} &\approx v \frac{\partial \phi}{\partial y} \end{aligned} \quad (6)$$

Using the approximations (6) in Equation 5 and substituting into Equation 4, the LHS is written:

$$\begin{aligned} \text{LHS} = \Delta x \Delta y \left\{ \phi_{i,j}^{n+1} - \phi_{i,j}^n + \frac{\Delta t \Delta x^2}{24} \left[ - u \frac{\partial}{\partial x} \left( \frac{\partial^2 \phi}{\partial x^2} \right) - v \frac{\partial}{\partial y} \left( \frac{\partial^2 \phi}{\partial x^2} \right) \right] \right. \\ \left. + \frac{\Delta t \Delta y^2}{24} \left[ - u \frac{\partial}{\partial x} \left( \frac{\partial^2 \phi}{\partial y^2} \right) - v \frac{\partial}{\partial y} \left( \frac{\partial^2 \phi}{\partial y^2} \right) \right] \right\} \quad (7) \end{aligned}$$

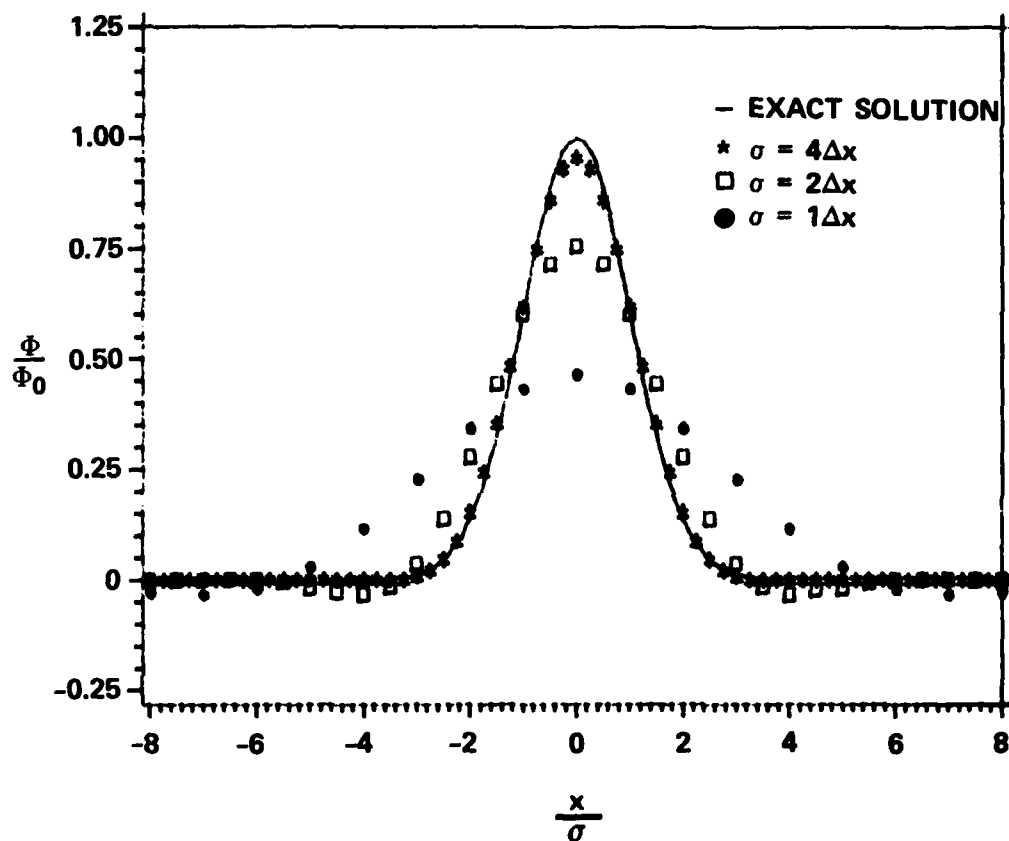


Figure 6. Effects of grid density on the unidirectional advection ( $C = 0.5$ ) of a Gaussian distribution

### Two-Dimensional Solid Body Rotation

36. The two-dimensional solid body rotation calculations were conducted using a symmetric bivariate Gaussian distribution of variance  $16(\Delta x)^2$  in a velocity field of constant angular frequency equal to  $\pi/1000 \text{ rad sec}^{-1}$ . Courant numbers defined at the center of mass of the distribution ranged from 0.34 to 0.01 which required 200 to 6400 time steps.

37. The results of the solid body rotation calculations are presented in Figures 7 and 8, which compare the simulation results of QUICKEST and 12-POINT with the exact solution, respectively. Examination of Figures 7 and 8 reveals that both 12-POINT and QUICKEST exhibit good phase and amplitude characteristics. However, unlike QUICKEST, whose control cell formulation ensures mass conservation, 12-POINT exhibited a 5 percent mass loss. This mass conservation error was subsequently investigated by repeating the test simulation with varying time steps. Figure 9, a plot of mass error, in percent, versus time

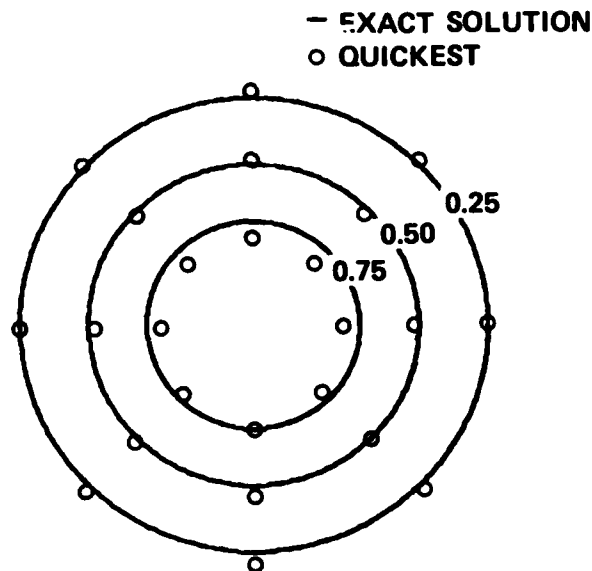


Figure 7. Comparison of QUICKEST with the exact solution for solid body rotation of a bivariate Gaussian distribution

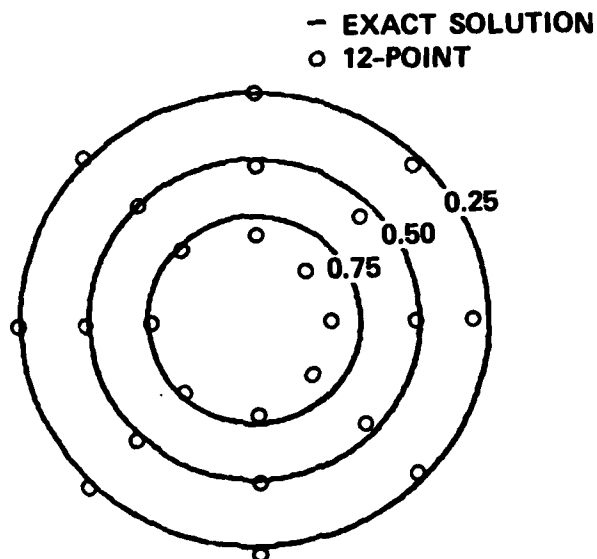


Figure 8. Comparison of 12-POINT with the exact solution for solid body rotation of a bivariate Gaussian distribution

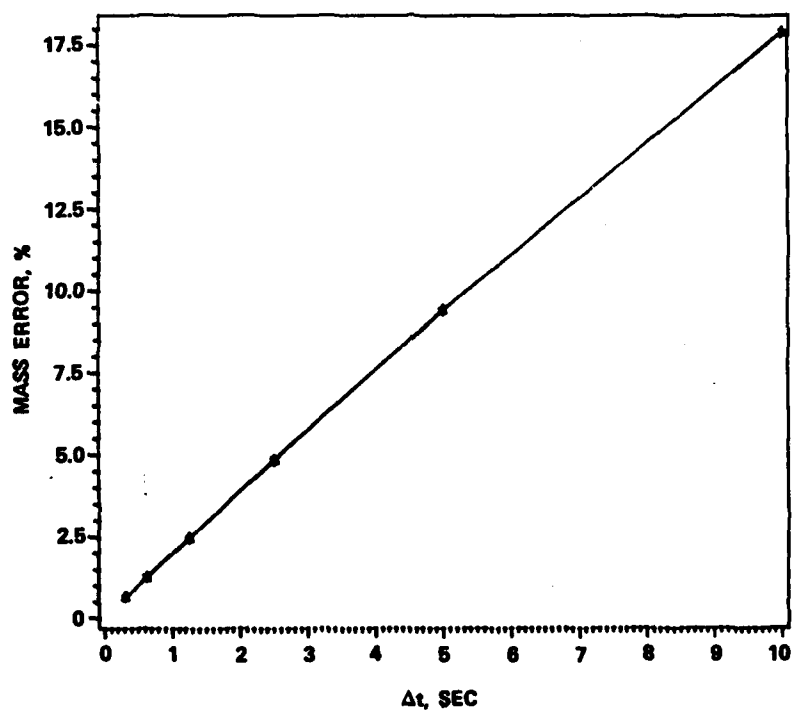


Figure 9. Mass conservation error of the 12-POINT scheme as a function of  $\Delta t$

step,  $\Delta t$ , clearly illustrates that the ability of 12-POINT to conserve mass is strongly dependent upon the time step employed. For completeness, the dependence of mass conservation error on grid density was investigated by decreasing the variance of initial Gaussian distribution to  $4(\Delta x)^2$ . The resulting difference in mass conservation error was less than 1 percent.

#### Neglect of the Cross-Derivative Terms

38. Solid body rotation experiments were conducted to investigate the effects of neglecting the cross-derivative terms in the formulation of the two-dimensional QUICKEST. Davis and Moore (1982) stated that the neglect of the cross-derivative terms had a negligible effect on the numerical results. The solid body rotation calculations were an extension of the previous two-dimensional test using all combinations of initial variances  $4(\Delta x)^2$  and  $16(\Delta x)^2$  and time steps 2.5 and 5.0 sec.

39. Figure 10 presents the comparison of QUICKEST with and without the cross-derivative terms at time steps of 2.5 and 5.0 sec with initial variances  $4(\Delta x)^2$  and  $16(\Delta x)^2$ . Examination of Figure 10 reveals that neglect of the cross-derivative terms results in increased diffusion/amplitude errors as grid density decreases or time step increases.

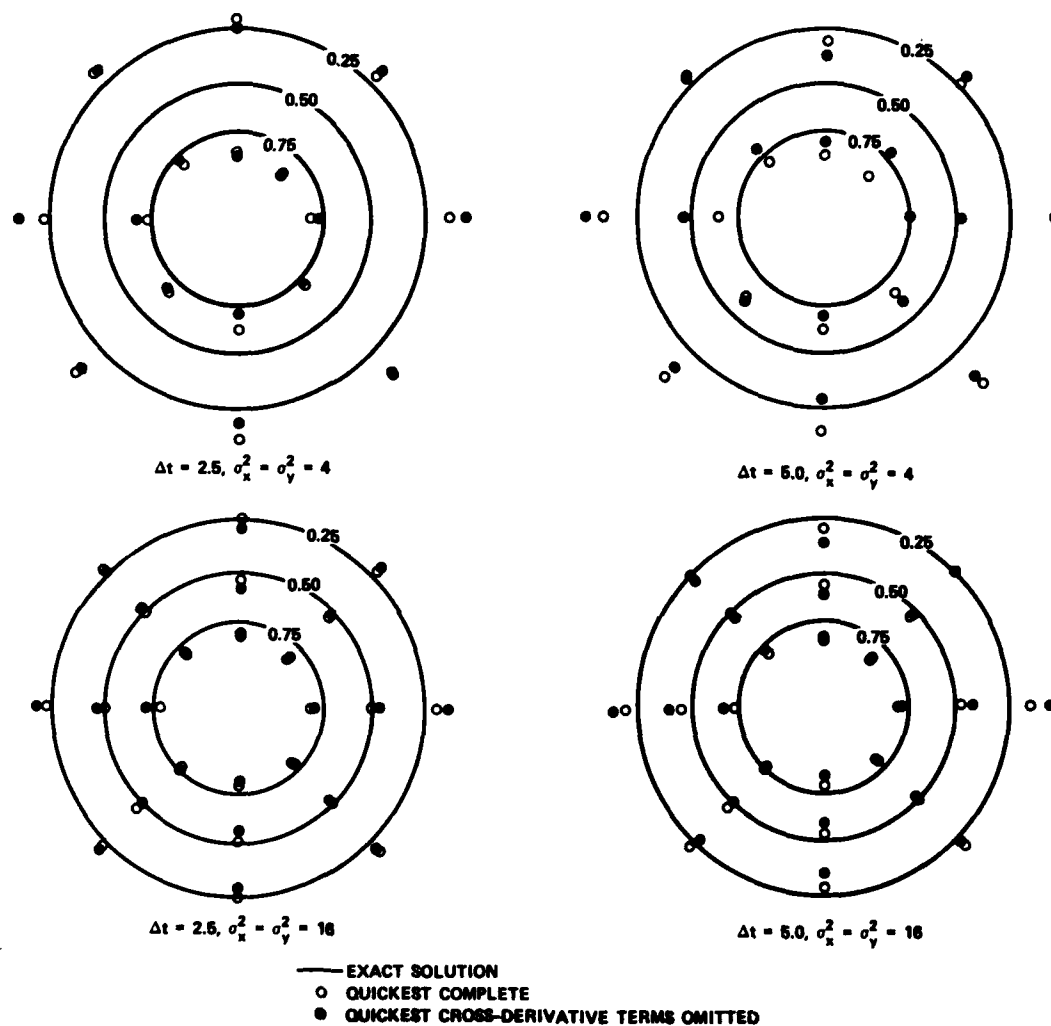


Figure 10. Comparison of QUICKEST with and without the cross-derivative terms at varying time steps and grid densities

## PART V: CONCLUSIONS

40. The purpose of this study was to detail the derivation of a two-dimensional QUICKEST and to compare its performance with 12-POINT, as applied to the solution of the advective transport equation. A systematic program of numerical experimentation was conducted for both one-dimensional and two-dimensional test cases.

41. Based on the results of the one-dimensional test case, it may be concluded that:

- a. QUICKEST and 12-POINT are algebraically equivalent for spatially constant Courant numbers.
- b. Variations in the Courant number result in small amplitude differences; however, simulations performed with varying grid densities show that inadequate grid resolution results in large amplitude errors.
- c. Phase errors are negligible.

42. The two-dimensional test results suggest that:

- a. Both QUICKEST and 12-POINT possess good phase and amplitude characteristics.
- b. Unlike QUICKEST, which conserved mass under all test conditions, the 12-POINT scheme exhibits a mass conservation error that varies directly with the size of the time step employed.
- c. Neglect of the cross-derivative terms results in increased diffusion/amplitude errors as grid density decreases or time step increases.

43. Finally, the work presented herein is preliminary to the development of a general purpose, depth-integrated water quality model. Realizing that the mass conservation property is a fundamental requirement, it is clear that, of the two third-order finite difference techniques examined, QUICKEST is far superior for engineering applications where practical grid spacing and time steps are essential.

## REFERENCES

- Chapman, R. S., and Kuo, C. Y. 1981. "Application of a High Accuracy Finite Difference Technique to Steady Free Surface Flow Problems," presented at the Joint ASME/ASCE Mechanics Conference, Boulder, Colo.
- Davis, R. W., and Moore, E. F. 1982. "A Numerical Study of Vortex Shedding from Rectangles," Journal of Fluid Mechanics, Vol 116, pp 475-506.
- Han, T. J., Humphrey, A. C., and Launder, B. E. 1981. "A Comparison of Hybrid and Quadratic-Upstream Differencing in High Reynolds Number Elliptic Flows," Computer Methods in Applied Mechanics and Engineering, Vol 29, pp 81-95.
- Hildebrand, F. B. 1956. Introduction to Numerical Analysis, McGraw-Hill, New York.
- Hinstrupt, P., Kej, A., and Kroszynski, U. 1977. "A High Accuracy Two-Dimensional Transport-Dispersion Model for Environmental Applications," Paper B17, 17th International Association of Hydraulic Research Congress, Baden-Baden, Germany.
- Leonard, B. P. 1979. "A Stable and Accurate Convective Modelling Procedure Based on Quadratic Upstream Interpolation," Computer Methods in Applied Mechanics and Engineering, Vol 19, pp 59-98.
- Leonard, B. P., Leschziner, M. A., and McGuirk, J. 1978. "Third-Order Finite-Difference Method for Steady Two-Dimensional Convection," Proceedings of the International Conference on Numerical Methods in Laminar and Turbulent Flow, Swansea, Wales.
- Leschziner, M. A. 1980. "Practical Evaluation of Three Finite Difference Schemes for the Computation of Steady-State Recirculating Flows," Computer Methods in Applied Mechanics and Engineering, Vol 23, pp 293-312.
- Leschziner, M. A., and Rodi, W. 1979. "Calculation of Strongly Curved Open Channel Flow," Journal of the Hydraulic Division, American Society of Civil Engineers, Vol 105, No HY10, pp 1297-1314.
- \_\_\_\_\_. 1981. "Calculation of Annular and Twin Parallel Jets Using Various Discretization Schemes and Turbulence-Model Variations," Journal of Fluids Engineering, Transactions, American Society of Mechanical Engineers, Vol 103, pp 352-360.

**END**

**FILMED**

**7-85**

**DTIC**